

Pharmacophore-Based Virtual Screening for Identification of Negative Modulators of GLI1 as Potential Anticancer Agents

Fabrizio Manetti,* Barbara Stecca,* Roberta Santini, Luisa Maresca, Giuseppe Giannini, Maurizio Taddei, and Elena Petricci*

Cite This: *ACS Med. Chem. Lett.* 2020, 11, 832–838

Read Online

ACCESS |

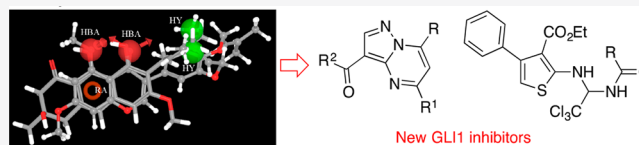
Metrics & More

Article Recommendations

Supporting Information

ABSTRACT: Starting from known GLI1 inhibitors, a pharmacophore-based virtual screening approach was applied to databases of commercially available compounds with the aim of identifying new GLI1 modulators. As a result, three different chemical scaffolds emerged that were characterized by a significant ability to reduce the transcriptional activity of the endogenous Hedgehog-GLI pathway and GLI1 protein level in murine NIH3T3 cells. They also showed a micromolar antiproliferative activity in human melanoma (A375) and medulloblastoma (DAOY) cell lines, without cytotoxicity in non-neoplastic mammary epithelial cells.

KEYWORDS: Pharmacophore-based virtual screening, Hedgehog pathway, GLI-1 modulators, anticancer agents, melanoma, medulloblastoma



Hedgehog (HH) signaling pathway plays a crucial role in embryonic cells differentiation and development, while it is usually deactivated in adults.^{1,2} An aberrant activation of HH pathway occurs in several so-called HH-dependent human cancers, such as basal cell carcinoma (BCC),³ medulloblastoma,⁴ meningioma,⁵ as well as in breast⁶ and colorectal cancers,⁷ and many others.⁸ The G protein-coupled receptor Smoothed (SMO) and the GLI transcription factors are the most promising targets for HH modulation. SMO remains the most investigated target for HH modulation⁹ with more than 18 compounds in preclinical studies (i.e., cyclopamine,¹⁰ CAT3,¹¹ MRT-92)¹² and active or completed clinical trials (i.e., taladegib,¹³ LEQ506).¹⁴ Four SMO inhibitors are already in the market for treatment of different cancers. Vismodegib and sonidegib are employed for treatment of advanced BCC, glasdegib for acute myeloid leukemia patients, and patidegib as an orphan drug for the treatment of basal cell nevus syndrome, as well as a topical gel formulation for sporadic nodular BCC.¹⁵ However, development of early resistance due to SMO mutations has been observed in many patients treated with vismodegib and sonidegib, thus limiting the efficacy of these drugs.¹⁶ On the other hand, the downstream effector GLI1 can be activated beyond SMO, overcoming its inhibition, and probably represents the most promising target to treat HH-dependent tumors avoiding resistance phenomena.¹⁷ The naturally occurring compounds vismione E¹⁸ and glabrescione B (GlaB)^{18–20} (Figure 1A) were recently described as inhibitors of GLI1 transcriptional activity, acting to a similar extent as GANT-61.²¹ However, a recent paper showed that the binding modes of GlaB and GANT-61 are significantly different.²²

The few GLI1 modulators known so far suffer from poor drug-like properties and activity, thus prompting the researchers to search for novel chemical entities. For this purpose, following a common feature pharmacophore generation approach implemented within the Phase software,²³ the two compounds were used to build a three-dimensional model that corresponded to the arrangement of their shared chemical portions. The resulting five-feature pharmacophore was constituted by two hydrophobic groups, two hydrogen bond acceptors, and one aromatic ring. They mapped the two terminal methyl groups of the *m*-prenyl side chain of GlaB and of the 7-prenyl group of vismione E, the oxygen atoms at positions 4 and 5 of GlaB and positions 8 and 9 of vismione E, the condensed phenyl ring of GlaB, and the central phenyl ring of vismione E, respectively (Figure 1B).

The pharmacophore was applied as a filter to virtually screen the Asinex and the AKos databases of commercially available compounds. As a result, among the 41 chemical entries prioritized by the virtual screening protocol, three structurally different hit compounds showed an interesting biological profile. Among them, α -mangostine (SST0673, a diprenylxanthone resembling GlaB in the prenyl side chains and the 5,7-dioxo-chromen-4-one core) showed a perfect superimposition to the pharmacophoric model. In particular, the oxygen atoms at positions 1 and 9 mapped the hydrogen bond acceptor

Special Issue: In Memory of Maurizio Botta: His Vision of Medicinal Chemistry

Received: December 21, 2019

Accepted: March 25, 2020

Published: March 25, 2020



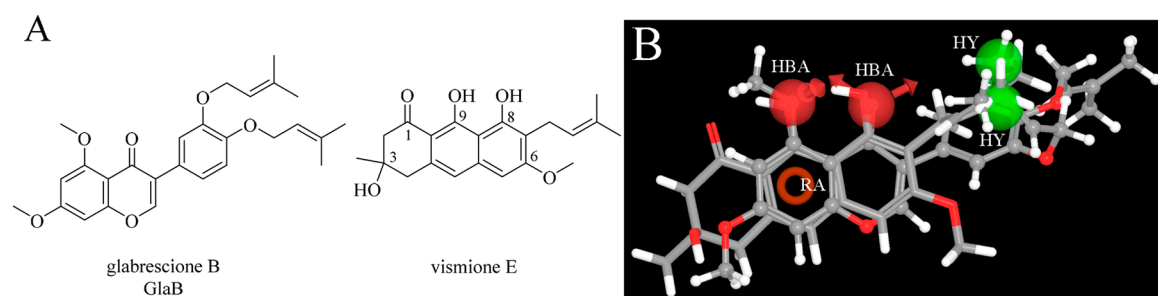


Figure 1. (A) Chemical structure of GlaB and vismione E used to generate the pharmacophore model for GLI1 inhibitors. (B) Graphical representation of the five-feature pharmacophoric model for compounds affecting GLI1 protein level. GlaB (ball and stick notation) and vismione E (stick notation) are superimposed. Green spheres are hydrophobic regions (HY); red spheres are hydrogen bond acceptor groups (HBA); the red ring is an aromatic ring feature (RA).

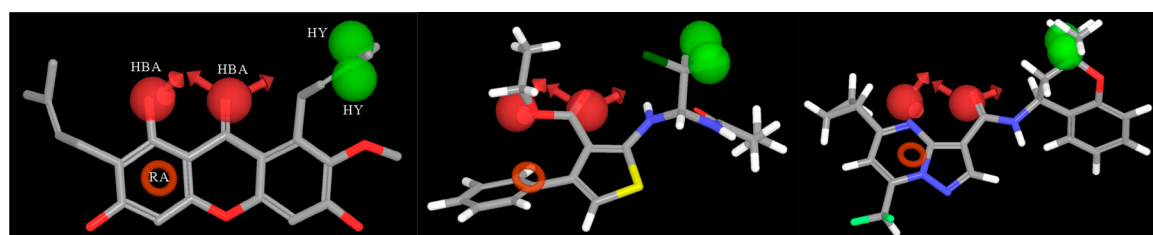


Figure 2. Graphical representation of the best-ranked superposition of α -mangostine (left), SST0683 (middle), and SST0704 (right) to the pharmacophoric model. Green spheres are hydrophobic regions (HY); red spheres are hydrogen bond acceptor groups (HBA); the red ring is an aromatic ring feature (RA).

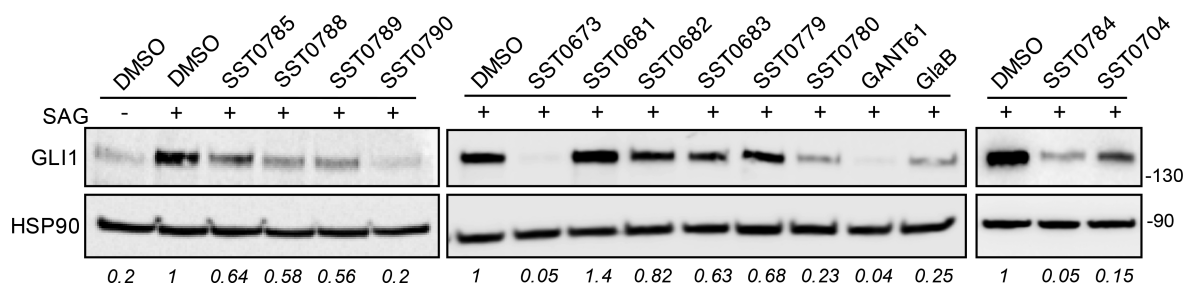


Figure 3. Effects of compounds on endogenous GLI1 protein level in NIH3T3 cells. Western blot analysis of GLI1 in cells treated with 100 nM SAG and DMSO, GANT-61, GlaB, or our putative GLI inhibitors (5 μ M) for 48 h. HSP90 was used as loading control. GLI1 protein quantification is indicated in italic.

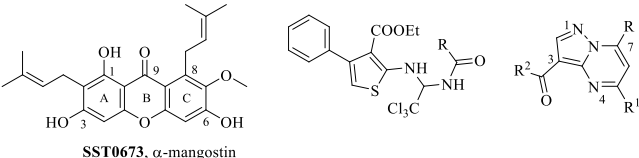
features (Figure 2, left), the methyl groups of the 8-prenyl appendage were the hydrophobic portions, and ring A fitted the aromatic ring feature.

The biological evaluation of SST0673 showed a significant reduction of GLI1 protein level in murine NIH3T3 cells treated with SAG (100 nM) (Figure 3). Moreover, about 43% inhibition was found in the luciferase assay in the same cell line, in comparison to SAG (100% luciferase activity, Table 1, Figure 4). Finally, this compound reduced cell proliferation at micromolar concentrations (2.7 and 1.9 μ M) in melanoma (A375) and medulloblastoma (DAOY) cell lines. Interestingly, the recent literature reports that α -mangostine may act as GLI inhibitor.^{24,25} This result provides experimental evidence that could support the reliability of the virtual screening protocol for the identification of putative GLI1 inhibitors.

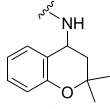
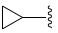
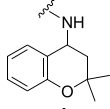
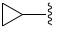
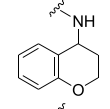
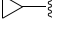
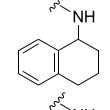
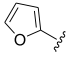
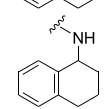
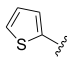
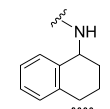
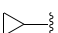
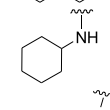
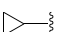
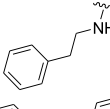
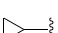
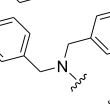

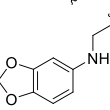
The second class of prioritized compounds was populated by thiophene derivatives (Table 1). Among them, SST0682 showed a reduction of GLI1 protein level and an antiproliferative activity in medulloblastoma cells significantly stronger (0.9 μ M) than in melanoma cells (12 μ M). The trichloromethyl group, the ester function, and the phenyl ring

at the thiophene represented the chemical features required to map the pharmacophoric model (Figure 2, middle). All these molecular portions were confirmed by molecular docking simulations as very important for the binding of SST0682 to GLI1 (Figure 5). Replacement of the phenyl ring at the amide terminus with an ethyl chain as in SST0683 maintained a micromolar antiproliferative activity (4.1 and 6.0 μ M), a reduction of GLI1 protein level, and 42% inhibition in the luciferase assay. Further size reduction of the terminal substituent to a methyl group led to SST0681 that did not affect GLI1 protein level, while it retained a micromolar antiproliferative activity (5.1 and 2.8 μ M). Moreover, changing the phenyl ring to the 2-furyl side chain led to SST0784, which strongly reduced the GLI1 protein level maintaining micromolar antiproliferative activity on cancer cells, while enlargement to a naphthyl moiety resulted in the inactive SST0781 (Table 1). Decoration of the phenyl ring with the electron-donating methyl group resulted in inactive compounds (SST0783, SST0767, and SST0768) independently from the substitution pattern. On the contrary, electron-withdrawing substituents, such as nitro (SST0780) and halogens (SST0785

Table 1. Structure and Antiproliferative Activity of Compounds That Affect GLI1



SST0673, α -mangostin

Compound	R	R ¹	R ²	Antiproliferative activity ^a		Effect on GLI1 protein ^b	Luciferase assay ^c
				A375	DAOY		
SST0673, α -mangostin				2.7±0.6	1.9±0.4	Strongly reduced	43
SST0681	Me			5.1±0.5	2.8±0.2	NA	38
SST0683	Et			4.1±0.5	6.0±0.6	Reduced	42
SST0682	Ph			12±1.3	0.9±0.1	Reduced	40
SST0783	<i>o</i> -Me-Ph			No activ.	No activ.	NA	ND
SST0767	<i>m</i> -Me-Ph			No activ.	No activ.	NA	ND
SST0768	<i>p</i> -Me-Ph			No activ.	No activ.	NA	ND
SST0779	<i>m</i> -Cl-Ph			6.1±0.6	5.5±0.3	Reduced	81
SST0780	<i>p</i> -NO ₂ -Ph			5.2±0.1	3.1±0.2	Strongly reduced	74
SST0785	<i>p</i> -Br-Ph			2.0±0.6	3.4±0.7	Reduced	78
SST0784	Furan-2-yl			2.7±0.1	4.3±0.2	Strongly reduced	51
SST0781	Naphth-1-yl			No activ.	No activ.	NA	7
SST0703	CHF ₂	Me		No activ.	No activ.	NA	0
SST0704	CHF ₂			2.2±0.5	2.3±0.4	Strongly reduced	40
SST0778	CHF ₂			No activ.	No activ.	NA	ND
SST0788	CHF ₂			5.0±0.4	7.5±0.4	Reduced	54
SST0789	CF ₃			0.6±0.1	5.7±0.9	Reduced	66
SST0790	CF ₃			1.2±0.5	4.4±0.5	Strongly reduced	49
SST0894	CHF ₂			ND	ND	NA	ND
SST0895	CHF ₂			ND	ND	NA	ND
SST0896	CHF ₂			ND	ND	NA	ND
SST0897	CHF ₂			ND	ND	NA	ND
GlaB				0.40±0.02	0.13±0.01	Strongly reduced	46

^aExpressed as IC₅₀ values (micromolar concentrations) calculated using GraphPad prism, version 6, from triplicate experiments in melanoma (A375) and medulloblastoma (DAOY) cells. ND: not determined. No activ.: no effects on proliferative activity. ^bGLI1 protein level was determined by Western blotting (see Figure 3 for details) in murine NIH3T3 cells treated with SAG (100 nM) and each compound (5 μ M) for 48 h. NA: not affected. ^cLuciferase assay in murine NIH3T3 cells. Data are represented as percentage of inhibition. Cells treated with SAG were equated to 100% (see Figure 4 for details). ND: not determined.

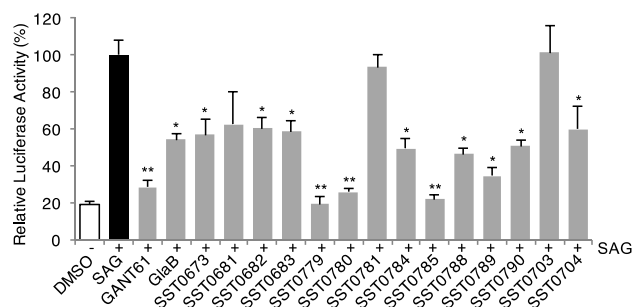


Figure 4. Effects of compounds on the transcriptional activity of the endogenous Hedgehog pathway. Quantification of GLI-dependent luciferase reporter assay in HH-responsive NIH3T3 cells treated with 100 nM SAG and the GLI inhibitors GANT-61, GlaB, or compounds (5 μ M) for 48 h. Relative luciferase activity was GLI-dependent reporter firefly/renilla control ratios, with cells treated with SAG equated to 100%. *, $p < 0.05$; **, $p < 0.01$.

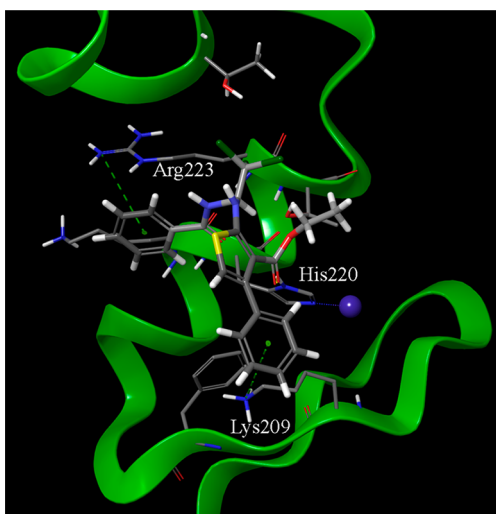


Figure 5. Best-ranked docking pose of the thiophene derivative SST0682. The phenyl rings at the amide spacer and at the thiophene nucleus are involved in π -cation interactions with the guanidino moiety of Arg223 and the ammonium group of Lys209, respectively. Moreover, the carbonyl oxygen of the ester side chain makes a hydrogen bond with His220 of the zinc chelating architecture. The trichloromethyl side chain is accommodated within the region occupied by the dimethyl moiety of SST0704 (Figure 6). The structure of SST0682 is represented by thick sticks, amino acid side chains by thin sticks, the zinc ion as a blue sphere, hydrogen bonds as dotted yellow lines, and π -cation interaction as dotted green lines.

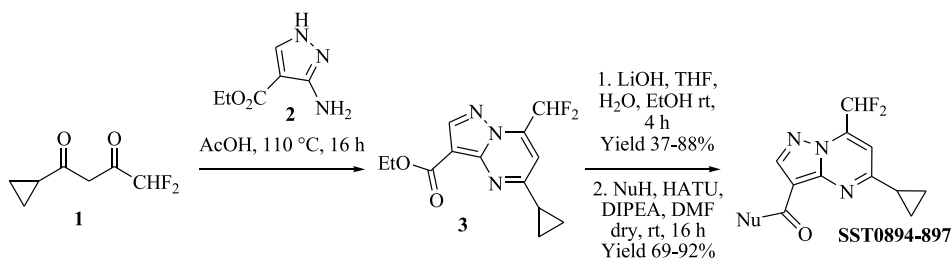
and SST0779), restored a micromolar antiproliferative activity, strongly affected luciferase assay (inhibition higher than 74%),

and reduced GLI1 protein level. As a representative example, SST0780 led to a >70% reduction of GLI1 protein level in comparison to SAG-treated cells (Figure 3).

Within the third class of hit compounds (Table 1), the pyrazolo[1,5-*a*]pyrimidine analogue SST0704 greatly decreased GLI1 protein level, inhibited the luciferase assay (by 40%), and showed a micromolar antiproliferative activity (2.2 and 2.3 μ M) in A375 and DAOY cell lines, respectively. In the attempt to rule SAR considerations on this class of compounds, several derivatives of SST0704 were synthesized or purchased from available commercial sources. The analogues SST0894–897 were synthesized by cyclization of the commercial 1-cyclopropyl-4,4-difluorobutane-1,3-dione **1** with pyrazole **2**, thus producing the ester **3**. It was converted, after saponification, into the corresponding pyrazolo[1,5-*a*]pyrimidines SST0894–897 in good yields and purity, by treatment with the appropriate amines in the presence of HATU as a coupling agent (Scheme 1). These analogs did not affect GLI1 protein level (Supporting Information Figure 1A) and, therefore, were not further characterized.

Replacement of the C5 cyclopropyl ring with a methyl group (SST0703) or removal of the *gem*-dimethyl substituent on the dihydro-chromene moiety (SST0778) led to inactive compounds that affected neither cell proliferation nor GLI1 protein level, thus suggesting an important role for both the C5 substituent and the hydrophobic dimethyl moiety on the chromene ring. Accordingly, docking simulations showed that the dimethyl assemblage, which was required to satisfy the hydrophobic features of the pharmacophoric model (Figure 2, right), pointed toward the polymethylene side chain of Arg223 (an essential amino acid for the interaction with DNA) and Thr243 (Figure 6). On the other hand, the cyclopropyl ring was directed toward the zinc binding site, possibly affecting the coordination of this ion. Simplification of the chromene core to a tetrahydro-naphthalene ring led to SST0788 that retained a micromolar antiproliferative activity (5.0 and 7.5 μ M) and showed a significant reduction of GLI1 protein and inhibition of the luciferase assay (54%). Although SST0788 lacked the dimethyl substitution on the chromene moiety, it gained a methylene fragment in place of the oxygen atom, which maintained the hydrophobicity that seemed required on this part of the molecule. Further manipulation of the appendage at the amide side chain led to inactive compounds (SST0894–SST0897). At the opposite molecular edge, insertion of small aromatic rings at C5 led to the most active pyrazolo-pyrimidine derivatives. In fact, SST0789 showed a micromolar antiproliferative activity (0.6 and 5.7 μ M) and a significant reduction of GLI1 protein level and luciferase activity (66%). Similarly, the corresponding thiophenyl analogue SST0790 showed an antiproliferative activity (1.2 and 4.4 μ M)

Scheme 1. Synthesis of Pyrazolo[1,5-*a*]pyrimidine Derivatives SST0894–897



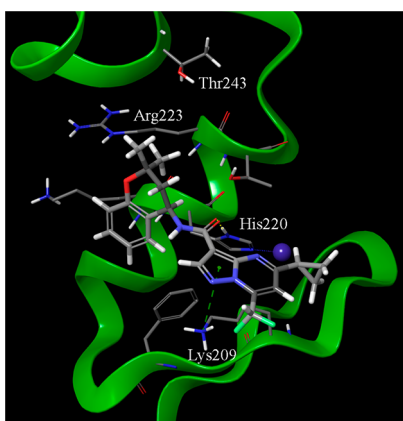


Figure 6. Best-ranked docking pose of SST0704 within GLI1 protein. Important interaction sites are represented by the pyrazole ring that gave a π -cation interaction with Lys209, the carbonyl group that is at hydrogen bond distance from His220 of the zinc binding pocket, the cyclopropyl ring that points toward the zinc binding pocket, and the *gem*-dimethyl moiety that is allocated between the side chains of Arg223 and Thr243. The structure of SST0704 is represented by thick sticks, amino acid side chains in thin sticks, the zinc ion as a blue sphere, hydrogen bonds as dotted yellow lines, and π -cation interaction as dotted green lines.

associated to an almost complete inhibition of GLI1 protein expression (Figure 3).

The hydrophobic character of pyrazolo-pyrimidines appeared to be a crucial parameter that affected compound activity. LogP values (calculated by MarvinSketch software, www.chemaxon.com) lower than 3.5 were associated to inactive compounds, while activity occurred in compounds with higher values, with the only exception SST0896 that was inactive with a logP value of 4.84.

The ability of such compounds to affect GLI1 protein level and inhibit luciferase assay suggested that they might interact with GLI1 itself. To support this hypothesis, molecular docking simulations (Glide software)²⁶ were performed on the X-ray structure of the five-finger GLI1/DNA complex (2gli within the protein data bank).²⁷ Best scored poses of GlaB showed that it accommodates in the region between zinc finger 4 and 5. Moreover, Lys209, Lys219, and Arg223 (we adopt amino acid numbering of the protein data bank even if a list to convert it into the full length numbering is reported in Supporting Information Table 1) make crucial interactions with GLI1 (Supporting Information Figure 2), as previously described.¹⁸ The agreement between the binding pose of docked GlaB and its major interactions within the GLI1

structure with those reported in previous literature gave further support to the reliability of the computational docking protocol. The latter was then applied also to thiophene and pyrazolo-pyrimidine hit compounds in the attempt to predict their binding mode and significant interactions with GLI1.

The thiophene derivative SST0682 was accommodated in such a way that the phenyl ring at the amide portion showed a cation- π interaction with the side chain of Arg223 (Figure 5), thus accounting for the importance of a phenyl ring at this position. Moreover, a similar interaction occurred between the phenyl ring on the thiophene cycle (corresponding to the aromatic ring feature of the pharmacophore) and the side chain of Lys209. Further stabilization came by a hydrogen bond between the ester side chain (that corresponds to an HBA feature of the model) and the His220 ring. The trichloromethyl group was embedded in a pocket comprised within the side chains of Thr224 and Thr243, where also the *gem*-dimethyl group of SST0704 was located (Figure 6).

The same binding pocket occupied by both GlaB and SST0682 also accommodated the pyrazolo-pyrimidine derivative SST0704 (Figure 6). In particular, the pyrazole ring gave a cation- π interaction with the terminal ammonium group of Lys209, and the amide oxygen of the ligand (that corresponds to one of the HBA features of the pharmacophore) interacted by hydrogen bond with the His220 heterocycle. Hydrophobic contacts involving both the chromene and the cyclopropyl rings further stabilized the complex. In particular, the latter pointed toward Cys207 that constituted the metal binding pocket for zinc ion of the zinc finger 4.

To further confirm the effects of these compounds on the GLI transcription factors, two pyrazolo-pyrimidines and two thiophene derivatives were selected to perform a gene expression analysis after treatment for 48 h at 5 μ M. Quantitative real-time PCR (qPCR) showed that all four compounds are able to reduce the expression of *GLI1*, *PTCH1*, *HIP1*, *GLI2*, and *Cyclin D1* mRNA (Figure 7). Similar results were obtained using GlaB. These results reinforce the effects of our compounds as GLI inhibitors.

To confirm the specificity of our compounds for GLI transcription factors, the effects of SST0683 and SST0790 on melanoma cell viability in GLI1- or GLI2-silenced A375 cells were also tested. This assay showed that depletion of GLI1 or GLI2 greatly attenuated the effects of our putative GLI inhibitors on cell viability, suggesting the specificity of our compounds for GLI1 and GLI2 (Figure 8). Finally, to exclude nonspecific cytotoxic effects, we demonstrated that the four selected compounds had no effect on cell viability in a non-neoplastic mammary epithelial cell line (MCF10A, Supporting

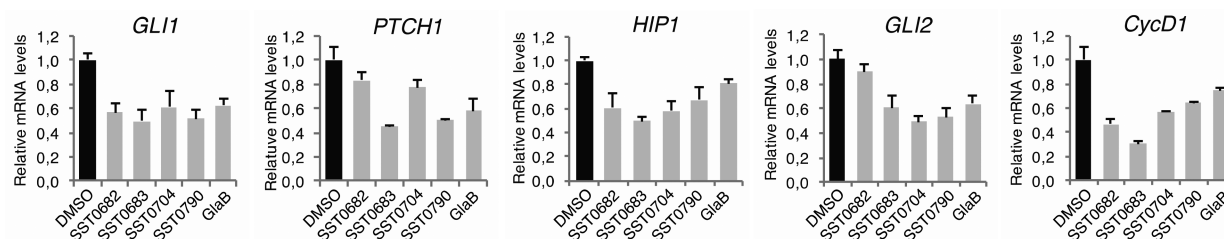


Figure 7. Gene expression analysis of Hedgehog pathway components upon treatment with compounds and GlaB. Quantitative PCR (qPCR) analysis of *GLI1*, *PTCH1*, *HIP1*, *GLI2*, and *Cyclin D1* in A375 cells treated with DMSO, SST0682, SST0683, SST0704, and SST0790 or GlaB (5 μ M) for 48 h. The y axis represents expression ratio of gene/(*HPRT* and *EIF2 α* average), with DMSO control equated to 1. Data shown as mean \pm SD.

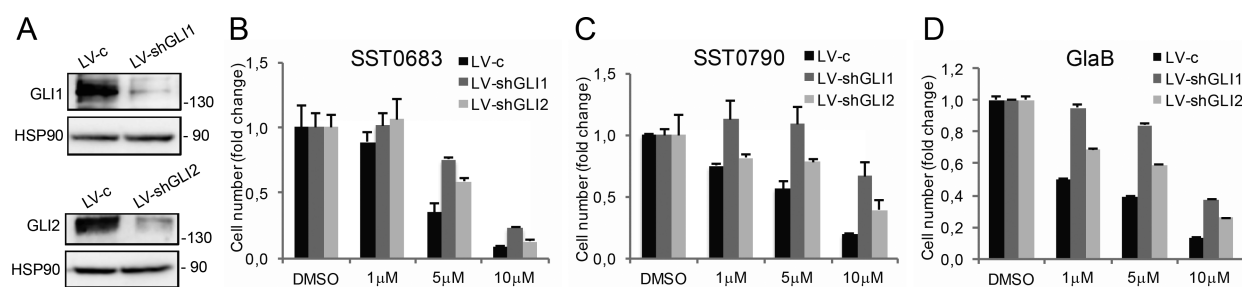


Figure 8. Silencing of GLI1 and GLI2 mitigates the effect of SST0683 and SST0790 on melanoma cell viability. (A) Western blot analysis of GLI1 and GLI2 in A375 cells transduced with LV-c, LV-shGLI1, or LV-shGLI2. HSP90 was used as loading control. (B–D) Effect of SST0683 (B) and SST0790 (C) on viability of A375 melanoma cells transduced as indicated. GlaB was used as a reference compound (D). Cells were treated with DMSO and compounds at the indicated doses for 72 h. Data are shown as mean \pm SD of at least three independent experiments.

Information Figure 1B), which expresses very low levels of GLI1 and of other HH pathway components and does not respond to HH pathway inhibition.²⁸

In conclusion, a pharmacophore-based virtual screening protocol led to discovery of three different chemical classes of compounds that reduced the transcriptional activity of the hedgehog-GLI pathway, affected GLI1 protein level, and showed antiproliferative activity toward both human melanoma and medulloblastoma cancer cells. They represent a good starting point for further steps toward a hit-to-lead process and, finally, a lead optimization phase up to the development of a new GLI1 negative modulator drug candidate.

■ ASSOCIATED CONTENT

Supporting Information

The Supporting Information is available free of charge at <https://pubs.acs.org/doi/10.1021/acsmchemlett.9b00639>.

Details of the computational protocols, synthetic procedures, analytical data, and conditions for biological assays. (PDF)

■ AUTHOR INFORMATION

Corresponding Authors

Fabrizio Manetti – Dipartimento di Biotecnologie Chimica e Farmacia, Università di Siena, I-53100 Siena, Italy; Lead Discovery Siena, I-53100 Siena, Italy; orcid.org/0000-0002-9598-2339; Phone: +39 0577 234330; Email: fabrizio.manetti@unisi.it

Barbara Stecca – Istituto per lo Studio, la Prevenzione e la Rete Oncologica (ISPRO), I-50139 Firenze, Italy; Phone: +39 055 7944567; Email: b.stecca@ispro.toscana.it

Elena Petricci – Dipartimento di Biotecnologie Chimica e Farmacia, Università di Siena, I-53100 Siena, Italy; Phone: +39 0577 234276; Email: elena.petricci@unisi.it

Authors

Roberta Santini – Istituto per lo Studio, la Prevenzione e la Rete Oncologica (ISPRO), I-50139 Firenze, Italy

Luisa Maresca – Istituto per lo Studio, la Prevenzione e la Rete Oncologica (ISPRO), I-50139 Firenze, Italy

Giuseppe Giannini – R&D, Alfasigma SpA, I-00071 Pomezia (Roma), Italy; orcid.org/0000-0002-7127-985X

Maurizio Taddei – Dipartimento di Biotecnologie Chimica e Farmacia, Università di Siena, I-53100 Siena, Italy; Lead Discovery Siena, I-53100 Siena, Italy

Complete contact information is available at:

<https://pubs.acs.org/doi/10.1021/acsmchemlett.9b00639>

Author Contributions

The manuscript was written through contributions of all authors. All authors have given approval to the final version of the manuscript.

Funding

This work was supported in part by a research grant from the AIRC foundation (grant IG 2017 Id 20758) and by the project “Development and application of QM/MM technologies for the design of light responsive proteins or protein-mimics based on rhodopsin architecture” within the program “Dipartimenti di Eccellenza -2018–2022 financed by MIUR (Roma, Italy). We are grateful for funding obtained from Istituto per lo Studio, la Prevenzione e la Rete Oncologica (ISPRO). Luisa Maresca is supported by a postdoctoral fellowship from Italian Association for Cancer Research (AIRC, project n. 22644). Additional financial support was provided by Leadiant Biosciences S.A. (Mendrisio, CH) (formerly Sigma-Tau Research Switzerland, S.A.). The MIUR research project 2015LZE994 (Insights into the functions of DNA damage processing and repair factors to design novel selective anticancer drugs), 2017SA5837 are also acknowledged.

Notes

The authors declare the following competing financial interest(s): G. Giannini participated in the project as Project Leader, thanks to the agreement signed between Leadiant Bioscience and Sigma-Tau IFR SpA (now Alfasigma SpA). Part of the results described herein have been the subject of a patent application: “GLI inhibitors and uses thereof” Application No EP 17166194.5 April 12, 2017. EP3388419A1. Giannini, G.; Taddei, M.; Manetti, F.; Petricci, E.; Stecca, B.

■ ACKNOWLEDGMENTS

The authors would like to thank G. Battistuzzi (R&D Alfasigma S.p.A., formerly Sigma-Tau IFR S.p.A.) for assistance with a few aspects of this project and A. Nosedà (Leadiant Biosciences SA) for facilitating this study. Glabrescione B was a gift from B. Botta and L. Di Marcotullio, University of Rome La Sapienza.

■ ABBREVIATIONS

HH, Hedgehog; SMO, Smoothed; BCC, basal cell carcinoma; HATU, hexafluorophosphate azabenzotriazole tetramethyl uranium; GlaB, glabrescione B.

REFERENCES

- (1) Ingham, P. W.; McMahon, A. P. Hedgehog signaling in animal development: paradigms and principles. *Genes Dev.* **2001**, *15*, 3059–3087.
- (2) Lum, L.; Beachy, P. A. The Hedgehog response network: sensors, switches, and routers. *Science* **2004**, *304*, 1755–1759.
- (3) Johnson, R. L.; Rothman, A. L.; Xie, J.; Goodrich, L. V.; Bare, J. W.; Bonifas, J. M.; Quinn, A. G.; Myers, R. M.; Cox, D. R.; Epstein, E. H., Jr.; Scott, M. P. Human homolog of patched, a candidate gene for the basal cell nevus syndrome. *Science* **1996**, *272*, 1668–1671.
- (4) De Souza, R. M.; Jones, B. R.; Lowis, S. P.; Kurian, K. M. Pediatric medulloblastoma - update on molecular classification driving targeted therapies. *Front. Oncol.* **2014**, *4*, 176.
- (5) Aavikko, M.; Li, S. P.; Saarinen, S.; Alhopuro, P.; Kaasinen, E.; Morgunova, E.; Li, Y.; Vesanen, K.; Smith, M. J.; Evans, D. G.; Pöyhönen, M.; Kiuru, A.; Auvinen, A.; Aaltonen, L. A.; Taipale, J.; Vahteristo, P. Loss of SUFU function in familial multiple meningioma. *Am. J. Hum. Genet.* **2012**, *91*, 520–526.
- (6) Bhateja, P.; Cherian, M.; Majumder, S.; Ramaswamy, B. The Hedgehog signaling pathway: a viable target in breast cancer? *Cancers* **2019**, *11*, No. E1126.
- (7) Gupta, R.; Bhatt, L. K.; Johnston, T. P.; Prabhavalkar, K. S. Colon cancer stem cells: potential target for the treatment of colorectal cancer. *Cancer Biol. Ther.* **2019**, *20*, 1068–1082.
- (8) Lospinoso Severini, L.; Quaglio, D.; Basili, I.; Ghirga, F.; Bufalieri, F.; Caimano, M.; Balducci, S.; Moretti, M.; Romeo, L.; Loricchio, E.; Maroder, M.; Botta, B.; Mori, M.; Infante, P.; Di Marcotullio, L. A Smo/Gli multitarget hedgehog pathway inhibitor impairs tumor growth. *Cancers* **2019**, *11*, 1518.
- (9) Bariwal, J.; Kumar, V.; Dong, Y.; Mahato, R. I. Design of Hedgehog pathway inhibitors for cancer treatment. *Med. Res. Rev.* **2019**, *39*, 1137–1204.
- (10) Taipale, J.; Chen, J. K.; Cooper, M. K.; Wang, B.; Mann, R. K.; Milenkovic, L.; Scott, M. P.; Beachy, P. A. Effects of oncogenic mutations in Smoothed and Patched can be reversed by cyclopamine. *Nature* **2000**, *406*, 1005–1009.
- (11) Chen, J.; Lv, H.; Hu, J.; Ji, M.; Xue, N.; Li, C.; Ma, S.; Zhou, Q.; Lin, B.; Li, Y.; Yu, S.; Chen, X. CAT3, a novel agent for medulloblastoma and glioblastoma treatment, inhibits tumor growth by disrupting the Hedgehog signaling pathway. *Cancer Lett.* **2016**, *381*, 391–403.
- (12) Vesci, L.; Milazzo, F. M.; Stasi, M. A.; Pace, S.; Manera, F.; Tallarico, C.; Cini, E.; Petricci, E.; Manetti, F.; De Santis, R.; Giannini, G. Hedgehog pathway inhibitors of the acylthiourea and acylguanidine class show antitumor activity on colon cancer in vitro and in vivo. *Eur. J. Med. Chem.* **2018**, *157*, 368–379.
- (13) Bendell, J.; Andre, V.; Ho, A.; Kudchadkar, R.; Migden, M.; Infante, J.; Tiu, R. V.; Pitou, C.; Tucker, T.; Brail, L.; Von Hoff, D. Phase I study of LY2940680, a Smo antagonist, in patients with advanced cancer including treatment-naïve and previously treated basal cell carcinoma. *Clin. Cancer Res.* **2018**, *24*, 2082–2091.
- (14) Peukert, S.; He, F.; Dai, M.; Zhang, R.; Sun, Y.; Miller-Moslin, K.; McEwan, M.; Lagu, B.; Wang, K.; Yusuff, N.; Bourret, A.; Ramamurthy, A.; Maniara, W.; Amaral, A.; Vattay, A.; Wang, A.; Guo, R.; Yuan, J.; Green, J.; Williams, J.; Buonamici, S.; Kelleher, J. F.; Dorsch, M. Discovery of NVP-LEQ506, a second-generation inhibitor of smoothed. *ChemMedChem* **2013**, *8*, 1261–1265.
- (15) Peer, E.; Tesanovic, S.; Aberger, F. Next-Generation Hedgehog/GLI pathway inhibitors for cancer therapy. *Cancers* **2019**, *11*, 538.
- (16) Pricl, S.; Cortelazzi, B.; Dal Col, V.; Marson, D.; Laurini, E.; Fermeglia, M.; Licitra, L.; Pilotti, S.; Bossi, P.; Perrone, F. Smoothed (SMO) receptor mutations dictate resistance to vismodegib in basal cell carcinoma. *Mol. Oncol.* **2015**, *9*, 389–397.
- (17) Pietrobono, S.; Gagliardi, S.; Stecca, B. Non-canonical Hedgehog signaling pathway in cancer: activation of GLI transcription factors beyond Smoothed. *Front. Genet.* **2019**, *10*, 556.
- (18) Infante, P.; Mori, M.; Alfonsi, R.; Ghirga, F.; Aiello, F.; Toscano, S.; Ingallina, C.; Siler, M.; Cucchi, D.; Po, A.; Miele, E.; D'Amico, D.; Canettieri, G.; De Smaele, E.; Ferretti, E.; Screpanti, I.; Uccello Barretta, G.; Botta, M.; Botta, B.; Gulino, A.; Di Marcotullio, L. Gli1/DNA interaction is a druggable target for Hedgehog-dependent tumors. *EMBO J.* **2015**, *34*, 200–217.
- (19) Ingallina, C.; Costa, P. M.; Ghirga, F.; Klippstein, R.; Wang, J. T.; Berardozi, S.; Hodgins, N.; Infante, P.; Pollard, S. M.; Botta, B.; Al-Jamal, K. T. Polymeric glabrescione B nanocapsules for passive targeting of Hedgehog-dependent tumor therapy in vitro. *Nano-medicine* **2017**, *12*, 711–728.
- (20) D'Alessandro, G.; Quaglio, D.; Monaco, L.; Lauro, C.; Ghirga, F.; Ingallina, C.; De Martino, M.; Fucile, S.; Porzia, A.; Di Castro, M. A.; Bellato, F.; Mastrotto, F.; Mori, M.; Infante, P.; Turano, P.; Salmasso, S.; Caliceti, P.; Di Marcotullio, L.; Botta, B.; Ghini, V.; Limatola, C. ¹H NMR metabolomics reveals the Glabrescione B exacerbation of glycolytic metabolism beside the cell growth inhibitory effect in glioma. *Cell Commun. Signaling* **2019**, *17*, 108.
- (21) Lauth, M.; Bergström, Å.; Shimokawa, T.; Toftgård, R. Inhibition of GLI-mediated transcription and tumor cell growth by small-molecule antagonists. *Proc. Natl. Acad. Sci. U. S. A.* **2007**, *104*, 8455–8460.
- (22) Calcaterra, A.; Iovine, V.; Botta, B.; Quaglio, D.; D'Acquarica, I.; Ciogli, A.; Iazzetti, A.; Alfonsi, R.; Lospinoso Severini, L.; Infante, P.; Di Marcotullio, L.; Mori, M.; Ghirga, F. Chemical, computational and functional insights into the chemical stability of the Hedgehog pathway inhibitor GANT61. *J. Enzyme Inhib. Med. Chem.* **2018**, *33*, 349–358.
- (23) Dixon, S. L.; Smondyrev, A. M.; Rao, S. N. PHASE: a novel approach to pharmacophore modeling and 3D database searching. *Chem. Biol. Drug Des.* **2006**, *67*, 370–372.
- (24) Verma, R. K.; Yu, W.; Shrivastava, A.; Shankar, S.; Srivastava, R. K. α -Mangostin-encapsulated PLGA nanoparticles inhibit pancreatic carcinogenesis by targeting cancer stem cells in human, and transgenic (Kras^{G12D}, and Kras^{G12D}/tp53R270H) mice. *Sci. Rep.* **2016**, *6*, 32743.
- (25) Ma, Y.; Yu, W.; Shrivastava, A.; Srivastava, R. K.; Shankar, S. Inhibition of pancreatic cancer stem cell characteristics by α -mangostin: molecular mechanisms involving Sonic Hedgehog and Nanog. *J. Cell. Mol. Med.* **2019**, *23*, 2719–2730.
- (26) Friesner, R. A.; Banks, J. L.; Murphy, R. B.; Halgren, T. A.; Klicic, J. J.; Mainz, D. T.; Repasky, M. P.; Knoll, E. H.; Shaw, D. E.; Shelley, M.; Perry, J. K.; Francis, P.; Shenkin, P. S. Glide: a new approach for rapid, accurate docking and scoring. 1. Method and assessment of docking accuracy. *J. Med. Chem.* **2004**, *47*, 1739–1749.
- (27) Pavletich, N. P.; Pabo, C. O. Crystal structure of a five-finger GLI-DNA complex: new perspectives on zinc fingers. *Science* **1993**, *261*, 1701–1707.
- (28) Zhang, X.; Harrington, N.; Moraes, R. C.; Wu, M. F.; Hilsenbeck, S. G.; Lewis, M. T. Cyclopamine inhibition of human breast cancer cell growth independent of Smoothed (Smo). *Breast Cancer Res. Treat.* **2009**, *115*, 505–521.